Estimation of Concentration and Load of Suspended Bed Sediment in a Large River by Means of Acoustic Doppler Technology

Francisco G. Latosinski[1]; Ricardo N. Szupiany[2]; Carlos M. García[3]; Massimo Guerrero[4]; and Mario L. Amsler[5]

Abstract: The standard experimental methods used for sampling suspended loads in large rivers are usually time consuming, unsafe, rather expensive, and have a limited spatial resolution. Acoustic Doppler current profilers (ADCPs), usually applied to measure the flow discharge, may also be used to assess the suspended sediment concentration by analyzing the backscattering acoustic strength. Though important efforts have been dedicated to test this method, results are not as reliable as engineering practices require, especially in large fluvial systems. In this paper, the correlation between the corrected backscatter from a 1,200 kHz ADCP and the suspended concentration from a depth-integrated sampler is presented and discussed. Despite the assumptions required to utilize this method (i.e., monosized grain and homogeneous vertical concentration), the results showed acceptable differences when they were compared with traditional methods. An evaluation of the backscatter and attenuation of sound produced by fine and coarse material is presented. Finally, the total suspended load of bed sediment is assessed using moving-boat ADCP measurements and compared with results from the corresponding standard method. Differences are at most 46%. **DOI: 10.1061/(ASCE)HY.1943-7900.0000859.** © *2014 American Society of Civil Engineers.*

Author keywords: Sediment transport; Acoustic techniques; Sampling; River systems.

Introduction

The quantification and understanding of the physical processes governing sediment transport in large rivers are of great scientific and technological interest for different disciplines. The sediment transported in the water column of a fluvial system, either from the riverbed (coarse material) or from the river basin (fine material), impacts in different ways on the behavior of the river, its habitat, and its uses (e.g., maintenance of hydropower-flood control reservoirs, inland waterways and ports, among others), hence the importance of understanding and accurately quantifying these physical processes.

The quantification of sediment transport in large streams is complex. The number and types of sediment samplers generally used to measure sediment transport in large rivers are limited. They could be classified in point or depth-integrated sediment samplers. Field experimental methods used to quantify sediment transport with these instruments require that the boat remains anchored at several river cross-sectional locations to vertically sample sediment concentration and flow velocity. Depth-integrated sediment samplers present some operational advantages in comparison with point samplers (i.e., shorter measuring time, lower number of sediment samples at each vertical, and shorter laboratory processing time, and, therefore, lower field and laboratory costs). Moreover, depth-integrated samples are of high interest for solid streamgauging (i.e., determination of solid fluxes), because errors due to vertical averaging are large when using a few point samples only. These factors lead to depth-integrated samplers being the most widely used samplers in large rivers. Although these methods are reasonably accurate (Gray et al. 2008; Gray and Simões 2008, Topping et al. 2011), they are too labor intensive, achieving low space and time resolution. These difficulties and shortcomings result in rare and scarce records for sediment transport in natural waterways, especially in large rivers around the world, as it is widely known that there are fewer sediment gauge stations than streamflow gauge stations. Therefore, it is necessary to measure sediment transport consistently and accurately, employing new experimental methods and techniques of feasible implementation in terms of information processing, associated costs, and spatial and temporal resolution.

The acoustic Doppler current profiler (ADCP), usually applied to measure flow discharge and flow velocity in river systems, is recognized as a potential tool for providing quantitative information on suspended sediment concentrations through the analysis of acoustic backscatter intensity. This technology has some advantages compared with the classical methods, because it is nonintrusive and a single measurement may be quickly performed from a

[1]Ph.D. Fellow, Concejo Nacional de Investigación Científica y Tecnológica, Facultad de Ingeniería y Ciencias Hídricas, Universidad Nacional del Litoral, Ciudad Universitaria, C.C. 217, RN° 168–Km. 472 (CP 3000), Santa Fe, Argentina (corresponding author). E-mail: franlatos@gmail.com

[2]Associate Professor, Facultad de Ingeniería y Ciencias Hídricas, Universidad Nacional del Litoral, Ciudad Universitaria, C.C. 217, RN° 168–Km. 472 (CP 3000), Santa Fe, Argentina. E-mail: rszupian@fich1.unl.edu.ar

[3]Associate Professor, Concejo Nacional de Investigación Científica y Tecnológica, Centro de Estudios y Tecnología del Agua, Laboratorio de Hidráulica, Facultad de Ciencias Exactas, Físicas y Naturales, Universidad Nacional de Córdoba, Av. Filloy s/n, Ciudad Universitaria (CP 5000), Córdoba, Argentina. E-mail: cgarcia2mjc@gmail.com

[4]Researcher, Hydraulic Laboratory, DICAM Dept., Bologna Univ., via Terracini (CP 40131) Bologna, Italy. E-mail: massimo.guerrero@unibo.it

[5]Researcher, Concejo Nacional de Investigación Científica y Tecnológica, Instituto Nacional de Limnología, Ciudad Universitaria, RN° 168–Km. 472 (CP 3000), Santa Fe, Argentina. E-mail: mamsler2003@yahoo.com.ar

Note. This manuscript was submitted on December 7, 2012; approved on December 9, 2013; published online on March 13, 2014. Discussion period open until August 13, 2014; separate discussions must be submitted for individual papers. This paper is part of the ***Journal of Hydraulic Engineering***, © ASCE, ISSN 0733-9429/04014023(15)/$25.00.

moving boat with high spatial and temporal resolution. Two types of approaches are available in the related literature using ADCPs for sediment transport quantification, both of them requiring knowledge of the nature of the suspended sediment (composition, size, shape, and concentration). One of them is based on knowledge of scattering particle acoustic properties (Holdaway et al. 1999; Thorne and Hanes 2002; Guerrero et al. 2012; among others). The other focuses on empirical expressions relating changes in the intensity of acoustic signals to simultaneously measured variations of particle concentration by applying standard, acoustic, or optical instrumentation (e.g., Gartner 2004; Topping et al. 2007; Szupiany et al. 2009; Moore et al. 2012; Sassi et al. 2012). Although these authors have reported encouraging results, the use of acoustic Doppler devices to measure sediment concentration and related suspended load requires further testing. In this sense, Sassi et al. (2012) review recent research advances in acoustic and sediment transport. The highly site-specific and seasonal dependence on ADCPs' backscatter calibrations appears to be one of the most complex problems with using this technology (e.g., Hoitink and Hoekstra 2005; Reichel and Nachtnebel 1994), which can be attributed to the sensitivity of the acoustic response to particle size, density, shape, and mineralogy (Moate and Thorne 2012) in the target volume.

Recent studies have focused on the influence of the suspended sediment in the attenuation of the acoustic signal intensity (e.g., Gartner 2004; Topping et al. 2007; Wright et al. 2010; Guerrero et al. 2011; Hanes 2012; Moore et al. 2012). This effect is strongly dependent on the characteristics of suspended particles, grain size, and concentration. Although Hoitink and Hoekstra (2005) found negligible attenuation, mainly due to low concentrations, Holdaway et al. (1999) found a 26% increase in the estimate of concentration when accounting for sediment attenuation. The quantification of sound attenuation due to suspended sediments is complicated in the presence of gradients in the concentration and variations in the size distribution of the suspended particles. This is particularly important in sand-bed rivers where lateral and vertical variation of concentration and grain size could be produced. For example, Topping et al. (2007), Wright et al. (2010), and Moore et al. (2012) included acoustic attenuation in their approaches estimating suspended mass concentration of fine material using horizontal ADCPs. However, their work assumes a uniform concentration field along the sound path. This behavior is something difficult or impossible to achieve in large sand-bed rivers.

The most complex effect on the backscatter and attenuation functions, given an instrument's working frequency, is the grain size distribution (Thorne and Meral 2008; Sassi et al. 2012; Guerrero et al. 2013). Sassi et al. (2012) introduce a simple approach that relies on at least two water samples along the sound path of the ADCP to obtain an empirically derived attenuation constant per unit concentration.

Despite the mentioned increasingly abundant literature on this promising technique, there are few studies showing its validity to estimate the sediment transport in large natural rivers, characterized by a reduced amount of appropriate/available equipment, complex/unsafe field procedures to sample suspended sediments, and lateral and vertical variability of grain size and concentration. In this sense, the paper aims to provide a detailed evaluation of acoustic signal-sediment concentration calibration and suspended bed-sediment transport computation with ADCP in a large sand-bed river (Parana River, Argentina) using a depth-integrated sediment sampler, the safest, most common, economical, and appropriate sediment sampler (among all kinds of available sediment samplers) used in large rivers.

Thus, this paper describes first the calibration and implementation of an experimental method used to estimate the suspended sand concentration (SSC) on the basis of the 1,200 kHz Teledyne-RDI ADCP records of backscattered signal. The calibration includes corrections of the ADCP records to account for the attenuation by beam spreading and fluid and sediment absorption. The experimental activities were performed in the main channel and a secondary stream of a large river, the Parana River, Argentina. ADCP measurements were simultaneous to the sampling of the sediment-laden water column by means of a depth-integrated sediment sampler. Finally, bed-sediment (sand) suspended load (Gss) was assessed by multiplying the flow velocity data by the concentration that was determined from the ADCP backscatter using the calibration curve. These results were compared with corresponding values derived from conventional methods, such as the equal width increment method.

Methods

Study Sites

The Parana River (Argentina) is the ninth largest river in the world in its mean annual flow discharge (Latrubesse 2008), with a drainage basin of 2.3×10^6 km^2 that includes parts of Brazil, Bolivia, Paraguay, and Argentina. Downstream of the major confluence with the Paraguay River (Fig. 1), the mean annual flow discharge of the Parana River is 19,500 m^3 s^{-1}, and the water surface slope is in the order of 1×10^{-5}. Alarcon et al. (2003) demonstrated, through measurements and careful calibration of transport formulas, that the average suspended sand load to bed load ratio is approximately 10 in the middle reach with values of Gss of 23×10^6 ton/year, while the washload sediment transport represents 91% of the total sediment transport. The Parana River planform pattern has been classified as anabranching with meandering thalweg (Latrubesse 2008). This multithread pattern forms a succession of wider and narrower nodal sections accompanied by a series of bifurcations and confluences around large midchannel bars, with mean channel widths and depths ranging from 600 to 2,500 m and 5 to 16 m, respectively.

The study sites are located in the middle and lower reaches of the Parana River and in the Colastine River (a secondary channel of the Parana River located at its middle reach): Zone A, near Lavalle City at the beginning of the middle reach; Zone B, near Parana City (in the middle reach); Zone C, Colastiné River near Santa Fe City; Zone D, near Rosario City in the upper part of the lower reach (see Fig. 1). In these zones, the bed material is composed almost completely of quartz sand (>90%), with small amounts of silt and clay (<4%) (Drago and Amsler 1998). These authors also report between 11 and 51% of very coarse and medium sand (mean grain size of 320 μm and geometric standard deviation, σ_g, of 1.43) in the middle reach between the cities of Corrientes and Rosario. Szupiany et al. (2012) present a first result of suspended and bed grain size distribution in the Parana River: this distribution is composed of well-sorted very fine sand (65%) and fine sand (35%) with a mean diameter of 94 μm ($\sigma_g = 1.4$). In addition, a grain size gap is observed by these authors between suspended and bed grain size sediment distributions, where only the finest grain size (from the bed) is in suspension.

Field Methods

Two different sets of measurements were performed at each site: fixed and moving-boat measurements. The flow depth was surveyed using a Raytheon single-beam echo sounder (SBES),

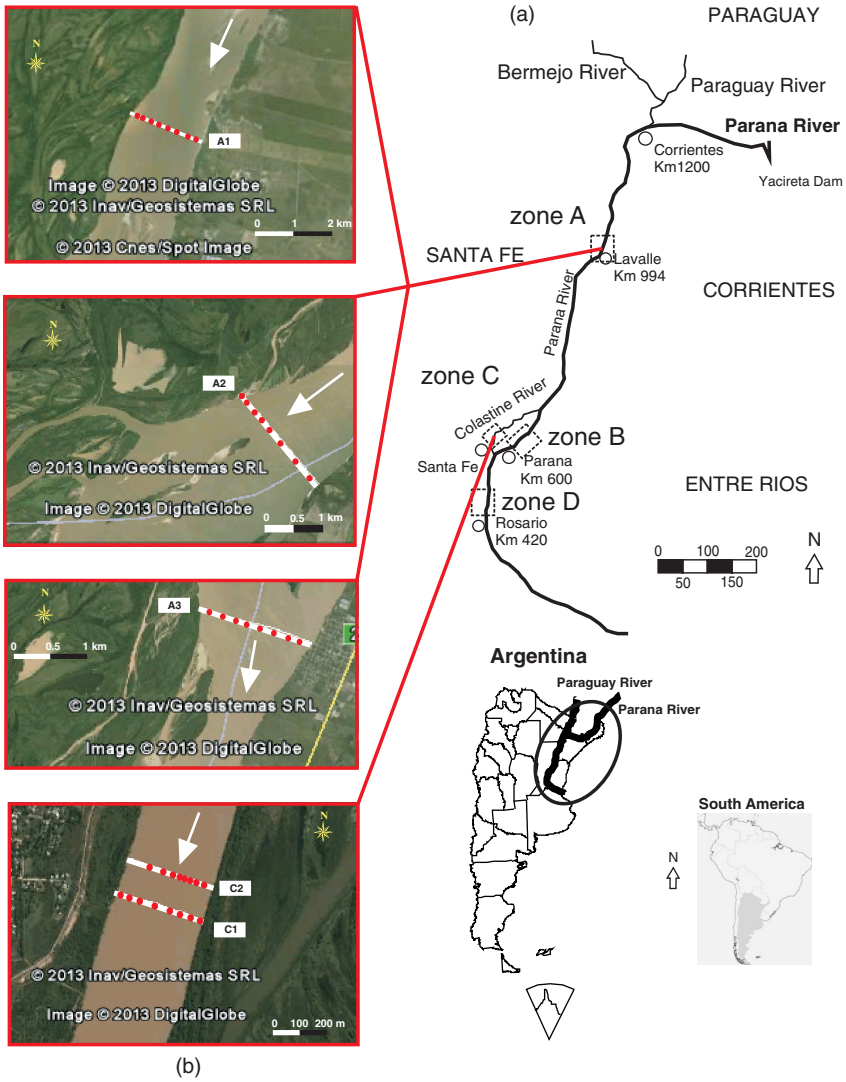

Fig. 1. (a) Study sites in the Parana River system (Szupiany et al. 2012, with permission from John Wiley and Sons); (b) River cross sections and locations for EWI method and ADCP profiling along the Parana River system (Map data: Google, Inav/Geosistemas SRL, DigitalGlobe, Cnes/SpotImage)

coupled to a differential global positioning system (DGPS), which was deployed on a small survey boat. A real-time-kinematic differential global-positioning-system (RTK DGPS) provided horizontal positions with an accuracy of ± 0.02 m at approximately 1 Hz. The flow velocity and the acoustic backscatter signal were measured with a 1,200 kHz ADCP manufactured by Teledyne RDI. Because the ADCP was deployed from a fixed and moving boat, it was linked to the RTK DGPS to provide both boat position and boat velocity. The bottom tracking function of the ADCP was not used to assess boat velocity because moving bed was observed at most of the verticals and across the studied river sections. In moving-boat measurements, the boat velocity and track position of the survey lines were monitored online by the helmsman, the velocity was maintained as constant as possible and lower than $\sim 1.5\ \mathrm{m\,s^{-1}}$ (for details see Szupiany et al. 2007). ADCP Water-Mode-1 was used to profile water velocity with a bin size of 0.25 m and about 0.5 s as ensemble time (no ping-to-ping averaging). ADCP compass calibration was made for all measurements involving the ADCP-DGPS (Teledyne RD Instruments 2007).

Fixed-Boat Measurements

For calibration purposes, a total of 36 different locations were surveyed in different flow field regions within study zones A, B, C, and D [Fig. 1(a)]. Zone A: eight verticals sampled on May 31, 2011 [across section A1, Fig. 1(b)]; Zone B: six verticals sampled on November 27, 2009; Zone C: two verticals sampled on October 30, 2009; eight verticals sampled on April 26, 2010 [across section C1, Fig. 1(b)] and eight verticals sampled on September 7, 2010 [across section C2, Fig. 1(b)]; and Zone D: four verticals sampled on November 16, 2010. The study sites in the Parana River system were as shown in Fig. 1(a): Zone A (near Lavalle City, upper reach); Zone B (near Parana City, middle reach); Zone C (near Santa Fe City, Colastine River); Zone D (near Rosario City, lower reach). Shown in Fig. 1(b) are river cross sections and locations for the EWI method and ADCP profiling along the Parana River system: Zone C, for two flow conditions, C1 and C2; and Zone A in three different sections and flow conditions at the Parana main channel, A1, A2, and A3. Table 1 shows the hydraulic characteristics (mean flow depth, h, and mean flow velocity, u) and total flow discharge, Q, at each measured zone. Water stage for each

Table 1. Mean Flow Velocity, Flow Depth, and River Flow Discharge at the 36 Selected Verticals

Zone	Vertical location	u ($m\,s^{-1}$)	h (m)	Q ($m^3\,s^{-1}$)
B	1	1.38	6.5	—
	2	1.34	9.2	—
	3	1.40	13	17,700[a]
	4	0.61	14.4	—
	5	0.66	9.2	—
	6	0.86	7.9	—
C	7	1.04	9.6	2,260[b]
	8	1.06	9.3	—
	9	0.79	7.3	—
	10	1.03	6.1	—
	11	0.98	6.8	—
	12	1.06	6.1	2,725[c]
	13	1.13	6.4	—
	14	1.01	8.3	—
	15	1.11	8.3	—
	16	1.10	9.3	—
	17	0.79	4.7	—
	18	0.82	4.7	—
	19	0.77	6.2	—
	20	0.82	6.7	1,620[d]
	21	0.81	4.3	—
	22	0.77	4.0	—
	23	0.83	5.9	—
	24	0.82	6.2	—
D	25	0.85	5.5	—
	26	0.65	4.5	14,320[e]
	27	0.94	6.1	—
	28	1.14	12.3	—
A	29	0.69	7.4	—
	30	1.01	9.7	—
	31	1.12	10.7	—
	32	1.11	9.0	17,921[f]
	33	1.11	12.5	—
	34	1.22	10.3	—
	35	1.08	9.5	—
	36	0.93	7.0	—

[a]November 17, 2009.
[b]October 30, 2009.
[c]April 26, 2010.
[d]September 7, 2010.
[e]November 16, 2010.
[f]May 31, 2011.

measured data set corresponded to medium and medium/low flow (Giacosa et al. 2000). The sampled range of concentrations (hydraulic conditions) was large enough to attempt to calibrate the backscatter signal versus concentration of suspended sediment. For each location, the sediment concentration in the water column was sampled by means of a depth-integrated isokinetic sampler, and at the same time ADCP measurements were performed. The sampler let us capture 5 L of sample; it had three different intake nozzles, diameters of 5, 7, and 9 mm, which were previously calibrated (isokinetic characteristic) according to the hydraulic conditions (Montagnini et al. 1998). So, for different ranges in mean flow velocities an appropriate nozzle diameter was selected. The maximum error observed between common flow condition in the Parana River and intake velocity was 15% (Montagnini et al. 1998). The influence of this error on the sediment concentration values depends on the suspended grain size (Guy and Norman 1970). For the common flow velocity range (i.e., recommended nozzle diameter of 7 mm) and suspended (sand) grain size at the Parana River, the maximum error in suspended sand concentration was expected to be 10% (Montagnini et al. 1998). Special care was taken with the integration time, which is related to the flow and intake velocities (see Fig. 1 in Gray and Gartner 2009). Thus, each sample (two-way depth integration) took between 2 and 4 min, depending on the depth and the current velocity. With the aim to compare samples with acoustic data, the vertically integrated samples did not include the near bottom zone which is not measured by the ADCP (i.e., about 6% of total depth) (Simpson 2001).

There exist other general sources of error that produced deviations from the mean suspended bed-sediment concentration value obtained with a depth-integrated sampler such as (a) bed contamination, (b) pressure-driven inrush, and (c) inadequate averaging time. Topping et al. (2011) demonstrated that the error arising from inadequate averaging time will likely be the dominant error introduced during the calibration of other approaches to measuring suspended sediment concentration. This error is produced by turbulent flow sediment fluctuation; therefore, it is site dependent. Further analysis should be made in future work in order to quantify the error produced by this factor on the Parana River and its secondary channels. For the present investigation, the measurements were performed with two-way depth integration and, as stated above, duration bigger than 1 min in order to reduce the error (Topping et al. 2011).

For suspended sediment transport purposes, five river cross sections [three in Zone A and two in Zone C, see Fig. 1(b)] were investigated for sand transport assessment by means of an isokinetic sampler (classical method). Eight locations in fixed positions at each cross section were sampled and ADCP profiled in order to obtain suspended sediment concentration and velocity data [see Fig. 1(b)]. The sampling process was the same as that described for calibration purposes.

Note that the samples obtained from sections A1, C1, and C2 were previously used for calibration purposes, corresponding to Zone A (from May 31, 2012, A1) and Zone C (from April 26, 2010, C1, and September 7, 2010, C2) (see Table 1). Thus, the remaining samples from cross sections A2 and A3 could be seen as components of independent data to verify the calibration.

Moving-Boat Measurements

Moving ADCP recordings along the five selected cross sections [Fig. 1(b)] was performed by tracking back and forth twice each cross section (i.e., four transect for each cross section) in order to filter out flow and concentration field variability. Dinehart and Burau (2005) and Szupiany et al. (2007) fully discuss this averaging process and the resulting ADCP measurement repeatability. Moreover, a first evaluation and comparison of the exposure time criteria for ADCP moving-boat discharge measurements (Oberg and Mueller 2007) and for ADCP moving-boat sediment transport measurements are presented.

Laboratory Procedures on Sediment Samples

Wet sieving, water evaporation, sediment drying, and weighing were performed for each sample to finally assess fine (i.e., silt and clay) and coarse (i.e., sand from the riverbed) sediment concentration in the sampled volume—that is, obtaining washload and suspended sand concentration data, respectively. Eight sand samples, two for each zone, were examined with a scanning electron microscope (SEM) to assess the grain size distribution and the major and minor axes (A and B, respectively) of individual grains. These axes were measured within the image plane. From each image, 50 grains were analyzed. Size distributions of silt and clay particles were investigated by Prendes et al. (2009) applying a

sedimentation method (hydrometers). Drago and Amsler (1988, 1998) observe that silt and clay size distribution is constant and homogeneous in the water column during the May to December period in the middle and lower reach of the Parana River. In the January through April period, they observe that the mean fine grain size decreases (more percentage of clay) while the annual concentration peaks provided by the Bermejo and Paraguay Rivers (upper Parana) take place (Fig. 1). These rivers supply more than 60% of the total washload at the Parana River in its middle reach (Drago and Amsler 1988). Note that all sediment data used in this investigation were sampled during the end of the April through December period.

Acoustic Backscatter Calibration

The ADCP used in the experiments described herein operates based on the same acoustic Doppler principles as all the instruments of this type that are commercially available, and it has similar restrictions. Thus, only some of its features, considered of interest to properly appraise the extent of the results, are given as follows. More information about basic principles of operation of ADCPs may be found in Simpson (2001).

As the pings transmitted by the transducers of a given ADCP move across the water depth, any suspended particles (sediments, air bubbles, or particulate organic matter) will scatter a certain part of the sound energy. Thus, the backscatter intensity will be related to the characteristics of the particles (i.e., with the concentration) present in the water column.

The backscatter intensity of the acoustic signal is a function of the equipment characteristics (acoustic frequency, transmitted power, measured volume range, received sensitivity) and the sediment transport conditions (concentration and size of sediment particles, amount of organic matter, dissolved solids, etc.). Therefore, for a given instrument and assuming a constant sediment type and size distribution and the absence of air bubbles and particulate organic matter, the signal strength would have a simple relation with the sediment concentration.

The acoustic model of scattering produced by the suspended particles is presented by different authors (Thorne and Hanes 2002; Gartner 2004; Wall et al. 2006; Wright et al. 2010; Guerrero et al. 2012; Hanes 2012, and others). This paper focuses on the basic equations to support the proposed methodology.

The starting point is the equation for the root mean square backscatter pressure from a suspension of scatters as a function of range (see details of the equation in Thorne and Hanes 2002). After some algebra and substitution, the typically referred sonar equation that relates backscatter signal to concentration of suspended sediment is commonly expressed in the logarithmic scale of decibel [Eq. (1)]:

$$\mathrm{RL} = \mathrm{SL} - 2\mathrm{TL} + 10\mathrm{Log}_{10}\left(f_S^2 \frac{\tau c}{a_S}\frac{M}{\rho_S}\right) + K_t \tag{1}$$

where RL = reverberation level (i.e., the received sound level in a nonisotropic environment); SL = source level; K_t = instrument-specific "system constant"; and TL = transmission losses. RL also corresponds to the ADCP recording in counts which are proportional to decibels (dB). The logarithmic expression denotes the target strength (i.e., the backscatter section of suspended spherical particles). In more detail, a_s = particle radius; τc = pulse length; M = mass concentration; ρ_s = particle density; and f_S = form function that describes the particle scattering properties.

Note that the backscatter term involves the particle radius and the form function. Thorne and Hanes (2002) empirically estimated the relation between f_S and the wave-number particle radius product, $x = ka_s$, using measurements of the acoustic backscatter from suspensions of sand-sized sediment, where $k = 2\pi/\lambda$ is the wave number and λ is the wavelength. For the 1,200 kHz frequency, particles with diameters ≥0.8 mm present a maximum f_S, while for values <0.8 mm, f_S decreases progressively [see Fig. 3(a) from Thorne and Hanes 2002].

Given a specific instrument and assuming a constant particle radius and speed of sound, the parameters SL, K_t, a_s, f_S, ρ_s, and τc can be included in a new constant K_T, therefore reducing Eq. (1) into (Thevenot et al. 1992)

$$\mathrm{Log}_{10}(M) = 0.1(\mathrm{RL} + 2\mathrm{TL}) + K_T \tag{2}$$

where the term RL + 2TL is the sum of ADCP backscatter's record, spherical acoustic beam spreading, and sound attenuation through the water column. The slope and intercept coefficient of the linear relation in Eq. (2) can be estimated by linearly fitting the logarithmic values of sampled concentration to the corrected acoustic signal (RL + 2TL). The slope coefficient may be compared to the 0.1 value; however, K_T is site and instrument properties dependent and must be calibrated.

The RL value in counts must be converted to decibels (dB) by means of transducer-specific scale factors. These constants are available on request from the manufacturer or can be assessed with a hydrophone test described in RD Instruments (1999). The mentioned factors for each ADCP beam used in this work are 0.3909, 0.4094, 0.4061, and 0.4120 for beams 1, 2, 3, and 4, respectively (Teledyne RD Instruments, personal communication, February 4, 2010).

The following equation is used for acoustic beam spreading and signal attenuation through the water column:

$$2\mathrm{TL} = 20\mathrm{Log}_{10}(\psi r) + 2\alpha_f r + 2\alpha_s r \tag{3}$$

where r = radial distance from the transducer; α_f = fluid absorption coefficient; and α_s = sediment absorption coefficient. The first term, $20\mathrm{Log}_{10}(\psi r)$, represents loss of acoustic signal strength due to beam spreading, and the second ($2\alpha_f r$) and third terms ($2\alpha_s r$) correspond to sound attenuation due to fluid viscosity and suspended particles, respectively. In Eq. (3), ψ is the correction coefficient for the transducer near the field zone because beam spreading is not linear in the near field and is estimated using Eq. (4) (Downing et al. 1995):

$$\psi = \frac{1 + 1.35z + (2.5z)^{3.2}}{1.35z + (2.5z)^{3.2}} \tag{4}$$

with

$$z = \frac{R\lambda}{\pi a_t^2} \tag{5}$$

and (Deines 1999)

$$R = r + \frac{H_B}{4} \tag{6}$$

where H_B = bin size; and a_t = transducer radius.

The sound absorption, α_f, in Eq. (3), for shallow freshwater mainly depends on acoustic frequency (f) and water temperature (T) and is computed in decibel per meter (dB/m) following Schulkin and Marsh (1962):

$$\alpha_f = \frac{29.36 \times 10^{-6} f^2}{f_T} \tag{7}$$

where $f_T = 21.9 \times 10^{[6-(1520/T+273)]}$, is the relaxation frequency dependent on T and T is in degrees Celsius (°C).

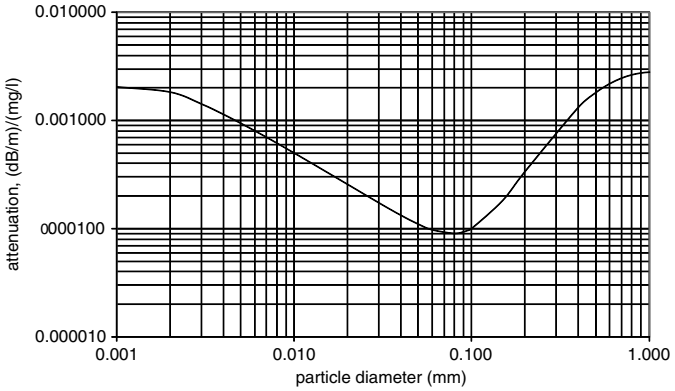

Fig. 2. Attenuation coefficient (α_s/M) due to sediments for the 1,200 kHz ADCP using Eq. (8)

The third term of Eq. (3) models acoustic absorption due to suspended particles. Eq. (8) gives the sediment attenuation coefficient (in dB/m) considering the viscous losses (first term) component (Urick 1948) and the scattering losses (second term) component (Thorne and Hanes 2002):

$$\alpha_s = 8.686 \cdot \left[\frac{k}{2}\frac{M}{\rho_s}(S-1)^2\left(\frac{s}{s^2+(s+\tau)^2}\right) + \frac{0.4}{D}\frac{M}{\rho_s}\left(\frac{x^4}{1+1.3x^2+0.24x^4}\right)\right] \quad (8)$$

where $S = \rho_s/\rho$ is the relative density; ρ_s is the sediment density; ρ is the fluid density; $s = (9/2\gamma D)[1 + (2/\gamma D)]$; $\gamma = \sqrt{\pi f/\nu}$; ν is the kinematic viscosity; $\tau = (1/2) + (9/2\gamma D)$; M is the sediment concentration; and D is the particle diameter. The R.H.S. first-term model is the viscous dissipation due to the relative motion between monosized spherical particles, and the second one represents the attenuation due to sediment scattering based on measurements made on sand-sized particles.

Note that in Eq. (8), the α_s coefficient depends on grain size and investigated unknowns (i.e., the sediment concentration). Thus, an iterative process is required to assess the concentration of suspended sediment also accounting for sound absorption due to sediment (Thorne and Hanes 2002; Guerrero et al. 2011). Given a sediment concentration, Fig. 2 shows the function of coefficient α_s for the 1,200 kHz ADCP and a particle size ranging between 0.001 and 1 mm. Considering the same concentration for fine and coarse material, it is clear that coefficient α_s presents the lowest value for a size around 80 μm.

In order to evaluate the different attenuation factors, four corrected signals were assessed: (1) CSB only accounts for beam spreading, (2) CSF also includes fluid sound absorption, (3) the sound attenuation due to fine material is further added in CSFM, and finally, (4) CSCM accounts for sound absorption due to coarse material. This is summarized in the following equations:

$$\text{CSB} = \text{RL} + 20\text{Log}_{10}\psi r \quad (9)$$

$$\text{CSF} = \text{RL} + 20\text{Log}_{10}\psi r + 2\alpha_f r \quad (10)$$

$$\text{CSFM} = \text{RL} + 20\text{Log}_{10}\psi r + 2\alpha_f r + 2\alpha_{sf} r \quad (11)$$

and

$$\text{CSCM} = \text{RL} + 20\text{Log}_{10}\psi r + 2\alpha_f r + 2\alpha_{sf} r + 2\alpha_{sg} r \quad (12)$$

where α_{sf} = attenuation coefficient due to the fine particles (clay and silt); and α_{sg} = attenuation coefficient due to the coarse sediment (sand). Both coefficients were computed considering the grain size and concentration for each fraction separately. The sum of both contributions yields the attenuation coefficient α_s.

Considering some assumptions, discussed below, the linear regression between the depth-integrated suspended bed-sediment concentration ($\overline{\text{SSC}}$) and the depth-averaged profiles of CSCM values ($\overline{\text{CSCM}}$) allows the instrument calibration to be obtained, provided that the fitting procedure approaches the theoretical slope of 0.1 [Eq. (2)].

Comparison between Sampling and ADCP Profiling Method for Suspended Load Assessment

Two methods for the assessment of suspended bed load were compared: the method that combines water column sampling with an independent velocity assessment in fixed vertical sections (i.e., the well-known equal width increment, EWI, method), and the moving ADCP simultaneous profiling of flow velocity and backscatter signal calibrated as described above.

Using the first method, the river cross sections were divided into eight subsections [see scheme in Fig. 3(a)] according to methodologies described by the World Meteorological Organization (WMO) (1994) and Gray et al. (2008). The cross section was divided into equal parts (EWIs) as constant as the complexity of the anchoring procedure permitted. For each subsection, the depth-averaged flow velocity was measured in the middle of each subsection using ADCP and at the same vertical point at which a depth-integrated isokinetic sampler was deployed. Then, subareas [i.e., Ω_i in Fig. 3(a)] of equal velocity and concentration [i.e., $\bar{U}_i$ and $\overline{\text{SSC}}_i$, respectively, in Fig. 3(a)] were assigned, and sediment discharge was computed as its product; finally, the products sum gave the suspended load for the entire cross section. In order to compare with the ADCP profiling method, the sampling was performed within the ADCP measurable range—that is, excluding the area near the riverbed where side lobe interference is produced [see Fig. 3(b)].

By the moving ADCP method, at least two complete (back-and-forth) surveys were performed (i.e., four transects were done at each river cross section, except at A3, where only two transects were performed). Therefore, the observed flow velocity and the acoustic raw signal were processed using the VMT software (Parsons et al. 2013) to finally assess time-averaged velocity and acoustic signal fields for the investigated cross section. The VMT software creates a homogenous grid where corresponding values of flow velocity and acoustic raw signal from the cross section can be averaged and then multiplied together. The calibration curve was then applied to estimate the sediment concentration (SSC) from the acoustic raw signal at each cell. Finally, the suspended load for the entire cross section was computed by integrating the flow velocity-SSC product over the computational grid schematically drawn in Fig. 3(b). The ADCP signal is not available near the water surface and margins because of the blanking distance and the low water depths, respectively. The suspended loads through near surface were estimated by extrapolation using a linear regression with information from the first (top) three valid cells. The edge sediment discharge was computed assuming a triangular area at the edge, through the methods widely accepted for flow discharge (Fulford and Sauer 1986).

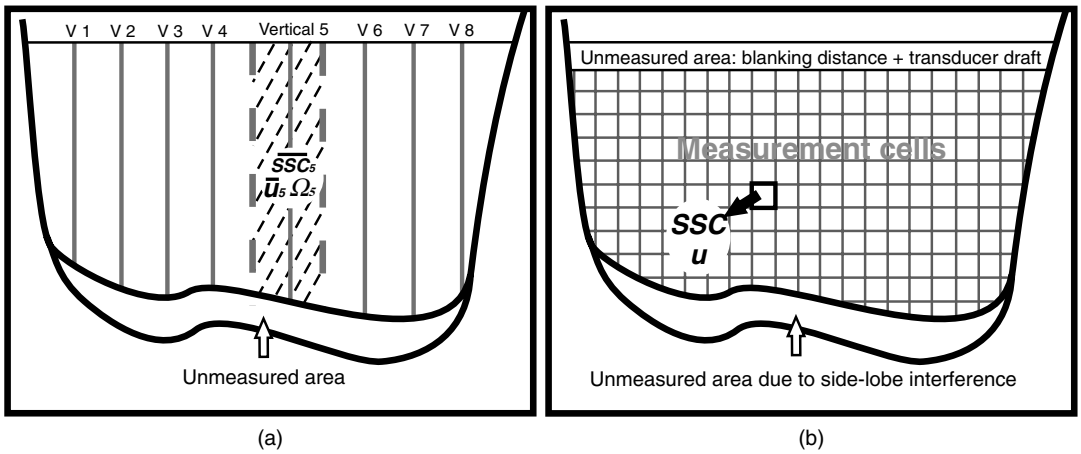

Fig. 3. Suspended load assessment using: (a) fixed sampling method; (b) moving ADCP profiling (adapted from Simpson 2001)

Results and Discussion

Suspended Sediment Characteristics

The depth-integrated concentrations of coarse (sand) and fine (silt and clay) fractions ($\overline{SSC}$ and $\overline{Cw}$, respectively) measured at the 36 fixed verticals are shown in Fig. 4. Note that values of $\overline{Cw}$ were within the range of 50–90% of the total concentration. Regarding suspended particulate organic matter, Szupiany et al. (2009) show that this variable presents concentrations lower than 0.1 mg L^{-1} for similar hydrological conditions, with a negligible effect on the acoustic signal. In addition, fine material flocculation does not take place in the Parana River main channel because of its relative high flow velocity, while it is observed in the floodplain of the Parana system (Mangini et al. 2003; Prendes et al. 2009).

Grain size distributions of suspended sand at different cross sections are shown in Fig. 5. Table 2 summarizes values of diameters D_{50}, D_{84}, D_{16} (50, 84, and 16% finer) and standard deviation, σ_g, of size distributions of suspended sand obtained for particle axes A and B. Values of σ_g clearly indicate the general uniformity of size distributions (see also Fig. 5). These results enabled using A-B averages in the calibrations.

Values of D_{50} and D_{84} equal to 5 and 25 μm, respectively, were taken for fine suspended particles (silt and clay) from the mean channel of the middle reach of the Parana River (Prendes et al. 2009). A uniform distribution of concentrations of fine material in the water column at each vertical was assumed (Drago and Amsler 1998) for calibration purposes.

Calibration Results

The fluid absorption coefficient α_f [Eq. (7)] computed neglecting pressure and salinity terms is 0.2974 dB/m. The sediment attenuation coefficient, α_s [Eq. (8)], was computed separately for fine and

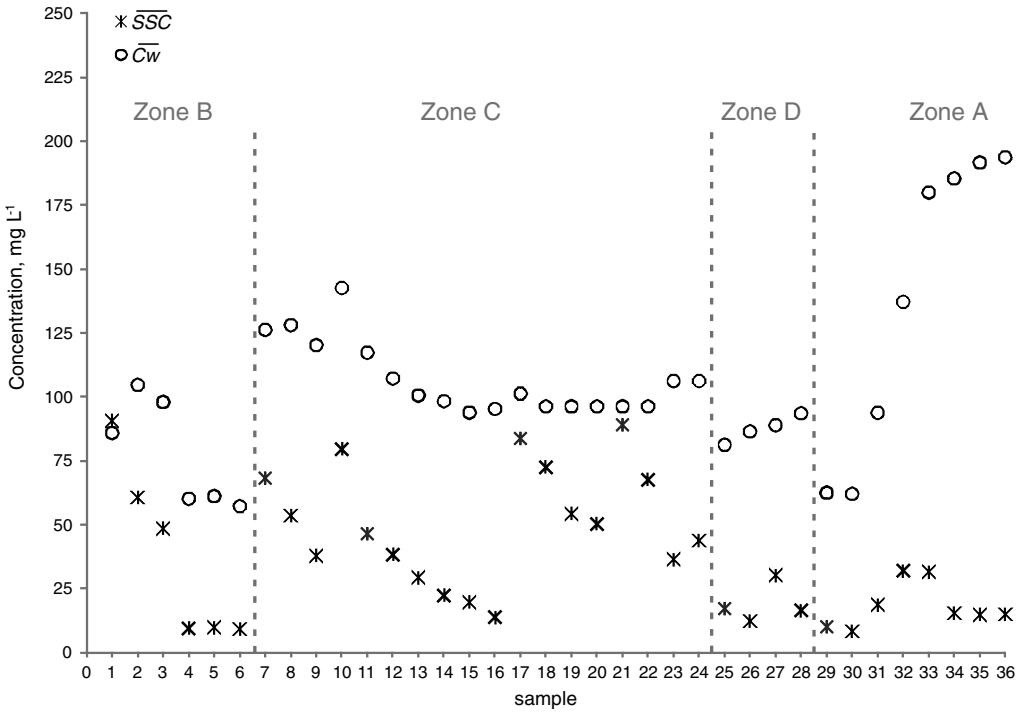

Fig. 4. Depth-integrated concentrations of coarse ($\overline{SSC}$) and fine ($\overline{Cw}$) suspended particles in the 36 fixed surveyed locations

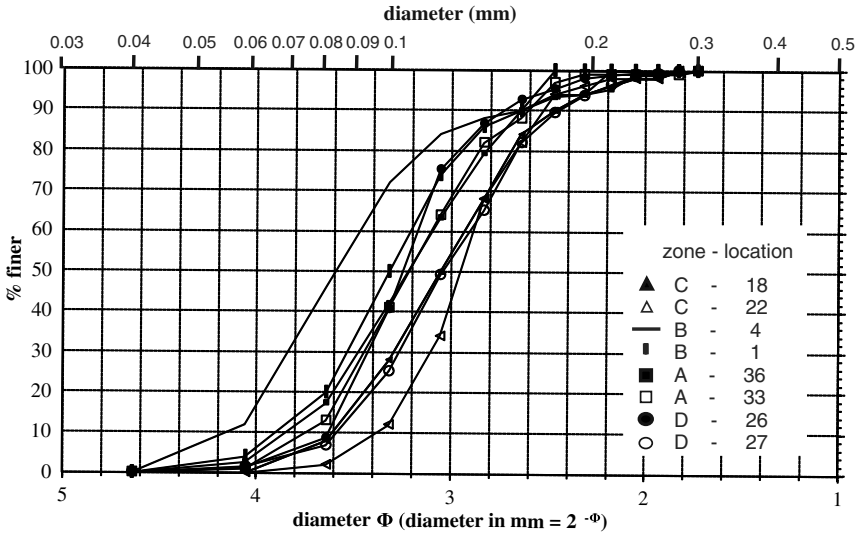

Fig. 5. Grain size distribution of the suspended sand (averages of axes A and B) sampled at different sections

Table 2. Typical Diameters from Size Distributions of Suspended Sand and Geometric Standard Deviation Computed for Axes A and B of Eight Samples Representative of Each Surveyed Zone

	D_{50}		D_{84}		D_{16}		σ_g	
	Axis							
Zone-location	A	B	A	B	A	B	A	B
C-22	129.4	82.5	163.8	116.6	106.6	33.5	1.2	1.9
B-4	98.1	70.6	134.0	96.4	76.9	48.0	1.3	1.4
C-18	120.7	81.1	159.3	112.7	89.9	54.4	1.3	1.4
B-1	83.9	63.4	120.7	85.4	63.6	42.0	1.4	1.4
D-26	104.4	78.5	130.1	100.5	87.5	56.3	1.2	1.3
A-36	107.0	80.6	143.6	109.4	79.7	58.3	1.3	1.4
D-27	124.4	90.4	165.2	117.9	95.0	66.4	1.3	1.3
A-33	104.4	81.2	159.4	109.2	83.3	64.0	1.4	1.3
Averages	109.0	78.5	147.0	106.0	85.3	52.9	1.3	1.4
Standard deviation	15.1	8.2	17.2	11.1	12.8	11.1	0.1	0.2
A and B averages	93.8		126.5		69.1		1.4	

Note: Mean values of axes A and B are plotted in Fig. 5 (values in μm).

coarse material (α_{sf} and α_{sg}) assuming monosized particle diameters equal to the corresponding D_{50} (5 and 94 μm, respectively) and homogeneous distribution along the water column. Values differed depending on sampling location, water depths, and fine and coarse sediment concentrations. Table 3 reports averaged values for all types of absorption coefficients.

Fig. 6 shows the corrections of the acoustic signal [Eqs. (9)–(12)] in percentage of $\overline{\text{CSCM}}$ at each of the sampled locations. Note the different relevances of each source of absorption/attenuation factors. See that the low values of α_{sf} and α_{sg} produced very small corrections with a maximum value of 1.4 and 0.07%, respectively, while water absorption and beam spreading gave rise to higher percentages with mean values of 2.7 and 11.4%, respectively.

The correlation between the depth-integrated coarse sediment concentrations ($\overline{\text{SSC}}$) and the depth-averaged corrected signal ($\overline{\text{CSCM}}$) is presented in Fig. 7. The equation of the regression line ($R^2 = 0.91$) is

$$\text{Log}_{10}(\overline{\text{SSC}}) = 0.121(\overline{\text{CSCM}}) - 8.798 \quad (13)$$

being $\overline{\text{SSC}}$ (in mg L^{-1}) and $\overline{\text{CSCM}}$ (in dB).

The slope coefficient of 0.121 is close to the theoretical value of 0.1 [Eq. (2)]. The scatter of the point data in Fig. 7 could be produced by different sources of errors such as (1) field and laboratory procedures and (2) assumptions of monosized sediment in the water column and across the cross section and homogeneous distribution of suspended sand concentration at each studied location (resulting from the depth-integrated sediment sampler). The next section further discusses these sources of errors. Nevertheless, the sources of errors mentioned, the intervals of $\pm 20\%$ encompass all the point data in Fig. 7 (i.e., a small variation for this type of estimation in alluvial rivers). Eq. (13) may be rewritten as

$$\overline{\text{SSC}} = 10^{[(0.121\overline{\text{CSCM}}) - 8.798]} \quad (14)$$

which is the expression used to compute the suspended sand concentration.

No correlation exists between fine sediment concentrations ($\overline{Cw}$) and the corrected signal ($\overline{\text{CSCM}}$; Fig. 8), although concentrations of fine sediment were two to ten times larger than the sand concentrations (Fig. 4). The substantially larger sensitivity of the

Table 3. Averaged Values of the Absorption Coefficients

Coefficient	α_f	α_s	α_{sf}	α_{sg}
dB m^{-1}	0.2974	0.065	0.061	0.004

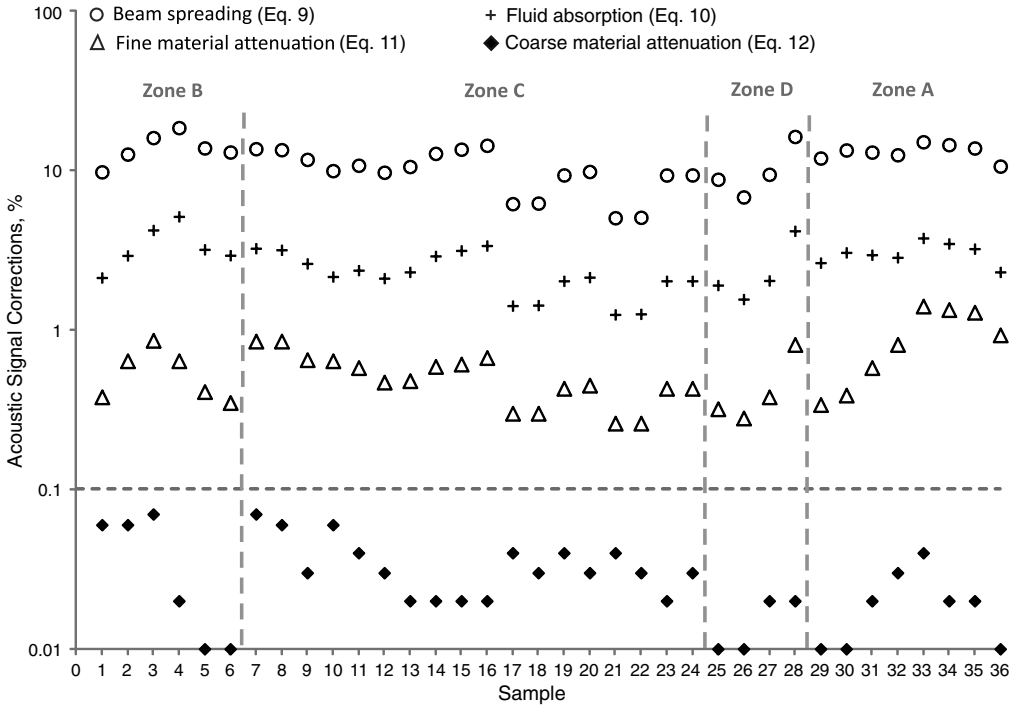

Fig. 6. Acoustic signal corrections as a percentage of $\overline{\text{CSCM}}$ [Eqs. (9)–(12)] at the 36 sampled locations used in the calibration

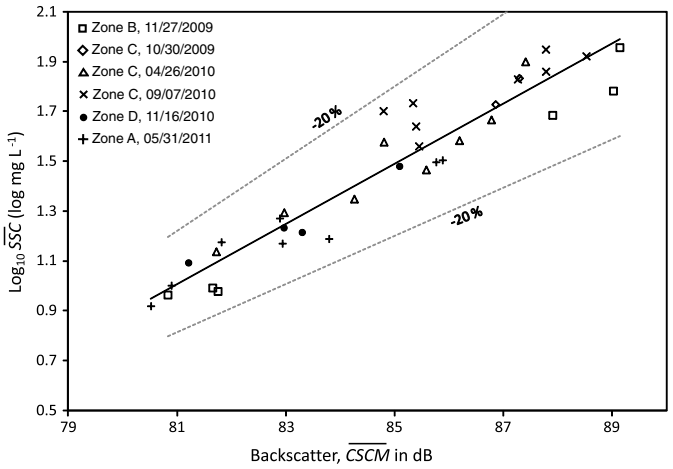

Fig. 7. Relationship between depth-integrated suspended sand concentration ($\overline{\text{SSC}}$) and depth-averaged corrected backscattered signal [$\overline{\text{CSCM}}$ in Eq. (12)]

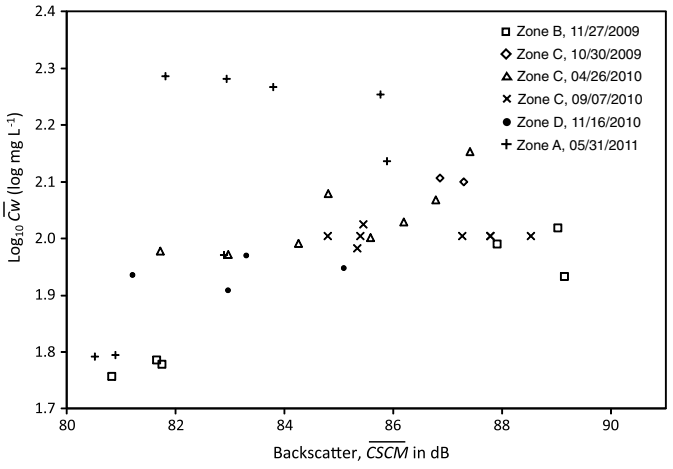

Fig. 8. Concentration of suspended fine sediment ($\overline{Cw}$) and corrected backscattered signal [$\overline{\text{CSCM}}$ in Eq. (12)]

corrected backscatter of sand particles for the applied working frequency (1,200 kHz) was already shown by Thorne and Hanes (2002) [Fig. 3(a)]. These authors show that the form function, f_S, is about 0.07 and 0.0002 for sand ($D_{50} = 0.094$ mm and $ka_s = 0.24$) and silt and clay ($D_{50} = 0.005$ mm and $ka_s = 0.012$), respectively. In spite of this small value on the form function, the washload could produce some scattering in the calibration curve presented in Fig. 7.

Errors in the Calibration Procedure

The sources of errors in the calibration procedure described above, responsible sources for the scatter in Fig. 7, could be grouped into (1) errors in sampling techniques due to the specific sampler used and current depth-integrated sampler; (2) laboratory procedure errors during sample analysis (concentration and grain size); (3) errors related to the sediment sampler that was used (i.e., homogeneous distribution of suspended bed-sediment concentration and monosized suspended bed sediment on the water column); and (4) errors due to the proposed assumption of linear relationship between depth-averaged values of $\overline{\text{CSCM}}$ and depth-integrated concentrations of suspended bed sediment over the water column. Note that two different ways of obtaining mean values have been used (depth integrated and depth averaged). Depth-averaged concentration is in general greater than depth-integrated concentration because the maximum values in flow velocity and sediment concentration are located in opposite regions of the water column. Sources of errors (1) and (2) present random behavior, and error

J. Hydraul. Eng.

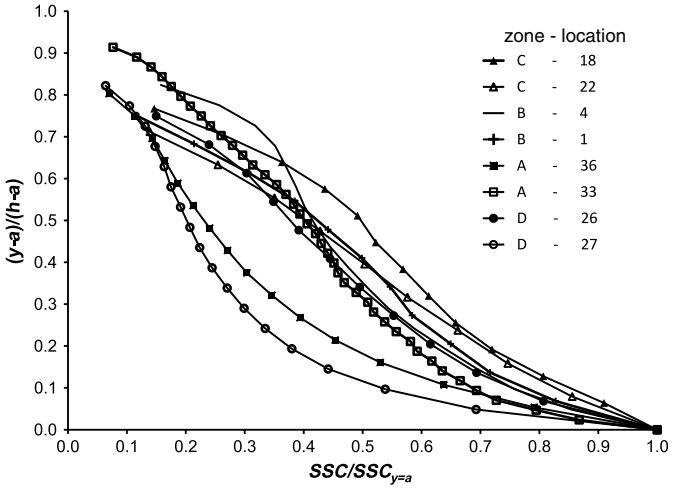

Fig. 9. Vertical distribution of suspended bed sediment concentration at the eight locations (see Tables 2 and 3 for more details)

Table 4. Validation of Suspended Bed Sediment Distribution in the Water Column Obtained from ADCP Calibration [Eq. (14)] through Rouse Formulation at the Eight Analyzed Verticals Presented in Tables 1 and 2

Zone-location	z (m)	R^2	a (m)	SSC$_{y=a}$ (mg L^{-1})	h (m)	u_* (m s^{-1})
C-22	0.4	0.97	0.82	129.3	4.0	0.05
B-4	0.4	0.98	1.09	75.6	6.2	0.05
C-18	0.4	0.99	0.83	149.1	4.7	0.05
B-1	0.5	0.99	1.03	197.4	4.7	0.04
D-26	0.5	0.99	0.80	24.8	4.5	0.04
A-36	0.7	1.00	0.86	64.1	5.5	0.03
D-27	0.7	0.97	0.90	136.9	6.1	0.03
A-33	0.5	0.96	1.63	52.4	12.3	0.04

source (4) represents bias errors. Regarding error source (3), considering a constant suspended bed-sediment concentration value in the water column in a "real" heterogeneous concentration profile (increasing from the water surface to the bed) will produce an overestimation on the sediment attenuation near the surface region producing higher signal intensity and, therefore, relative concentrations. This source of error will produce an underestimation of sediment attenuation near the bed region, and therefore, will produce smaller signal intensity and sediment concentrations. The same analysis could be done considering "the real" grain size evolution through the water column, which is well known for sand-bed rivers (i.e., grain size decreasing from the bed to the surface). Assuming monosized suspended bed sediment will produce an underestimation of the sediment attenuation near the bed (where largest real grain size should be present), smaller signal intensity and estimated concentration can be predicted. Note that in Fig. 2 grain sizes larger than the mean sand value (94 μm) will produce the highest attenuation. For smaller bed grain size, in the range between 94 and 62 μm (as is expected near the surface zone), the attenuation coefficient remains approximately constant. Therefore, both effects (assumptions of homogeneous concentration and monosized sediment distribution) act in a similar manner near the bed zone (underestimation of concentrations), while near the surface region the calibration will tend to overestimate the sediment concentration.

For ranges in grain size and concentration involved in this study case (Table 2 and Fig. 4), the well-sorted suspended bed sediment presented at all locations and the small bed-sediment attenuation effect (Fig. 6) suggest that the assumptions described above will not introduce significant errors in the results. Moreover, as shown in Fig. 5 and Tables 1 and 2 (see location and hydraulic characteristics, i.e., depth and mean velocity, of the eight suspended sediment samples analyzed for grain size distribution), it can be seen that even though the morphology and hydraulic conditions change significantly, the grain size distribution remains approximately constant with mean deviations, σ_g, ~1.4. The grain size corresponds to very fine and fine sand. As a first approach, there are not significant variations of suspended bed-grain size distribution on the water column and across the width of the stream. Distributions of Fig. 5 are the first published in the Parana River, and more analyses should be done in future studies, especially during high water levels (not measured at the moment). The use of a point sampler should be considered in future investigations to accurately evaluate/quantify the effect of these assumptions.

In order to check and demonstrate that the bias error [i.e., points (3) and (4), see above] could not be a significant error for the calibration and the application processes, the Rouse equation (Vanoni 1975; García 2008) was applied to obtain the mean shear velocity at the eight vertical locations where particle sizes of suspended bed-sediment samples were analyzed (Fig. 9, see also Tables 1 and 2 for the characteristics of each vertical location). The plot in Fig. 9 was prepared according to the Rouse formulation (see Vanoni 1975). Since ADCP cannot measure near the surface zone, values of the y-axes do not start at 1 in Fig. 9. The notation SSC$_{y=a}$ is the concentration at a distance a from the bed; and a is the distance from the bed to the first ADCP measured cell. The Rouse equation has been found to work well in several large rivers and has been recognized as a method to obtain shear velocity if grain size is known (García 2008).

Due to variations on bed morphology (bed composed by dunes) and complex planform geometry (i.e., a succession of wider and narrower nodal sections accompanied by a series of bifurcations and confluences around large midchannel bars), shear velocities were compared to reported mean values (Trento et al. 1990; Szupiany et al. 2012) and not to local values at each vertical location. The vertical distributions of suspended bed-sediment

Table 5. Comparison of Mean Suspended Bed Sediment Loads ($\overline{\text{Gss}}_m$) Computed with Sampling and ADCP Profiling Methods at Different Cross Sections and Discharges

			$\overline{\text{Gss}}_m$ (kg s^{-1})		
Date (m/d/y)	Discharge (m^3 s^{-1})	Location	Sampling method	ADCP profiling method	Deviation (%)
04/26/10	2,607	C–C1	80	70.4	−12.0
09/08/10	1,650	C–C2	56	48.2	−14.0
05/31/11	17,921	A–A1	320	468.6	+46.3
07/20/11	18,753	A–A2	507	554.0	+9.3
08/24/11	23,346	A–A3	1,070	1,240.1	+15.9

Note: The $\overline{\text{Gss}}_m$ values from the ADCP profiling method were derived from four averaged transects at each date. (The A3 result was derived from only two averaged transects.)

concentrations were obtained applying Eq. (14) and then plotted in log-log scales as suggested by Vanoni (1975) (Fig. 9). The slope of each linear regression is the Rouse exponent, z. Thus, if the representative size of suspended sediment is known (i.e., particle fall velocity), the bed-shear stresses can be obtained.

The values of z and shear velocities, u_*, obtained with the above procedures are presented in Table 4. Note that the reference level, a (and its associated concentration), corresponded to the first valid cell measured by the ADCP above the bed. In all cases, the determination coefficient, R^2, is higher than 0.96. The values of the u_* ranged from 0.03 to 0.05 m s^{-1} in agreement with common mean values of shear stresses in the Parana River (e.g., Trento et al. 1990; Szupiany et al. 2012). These results were obtained within a rather ample range of flow velocities, depths, and discharges (see Table 1),

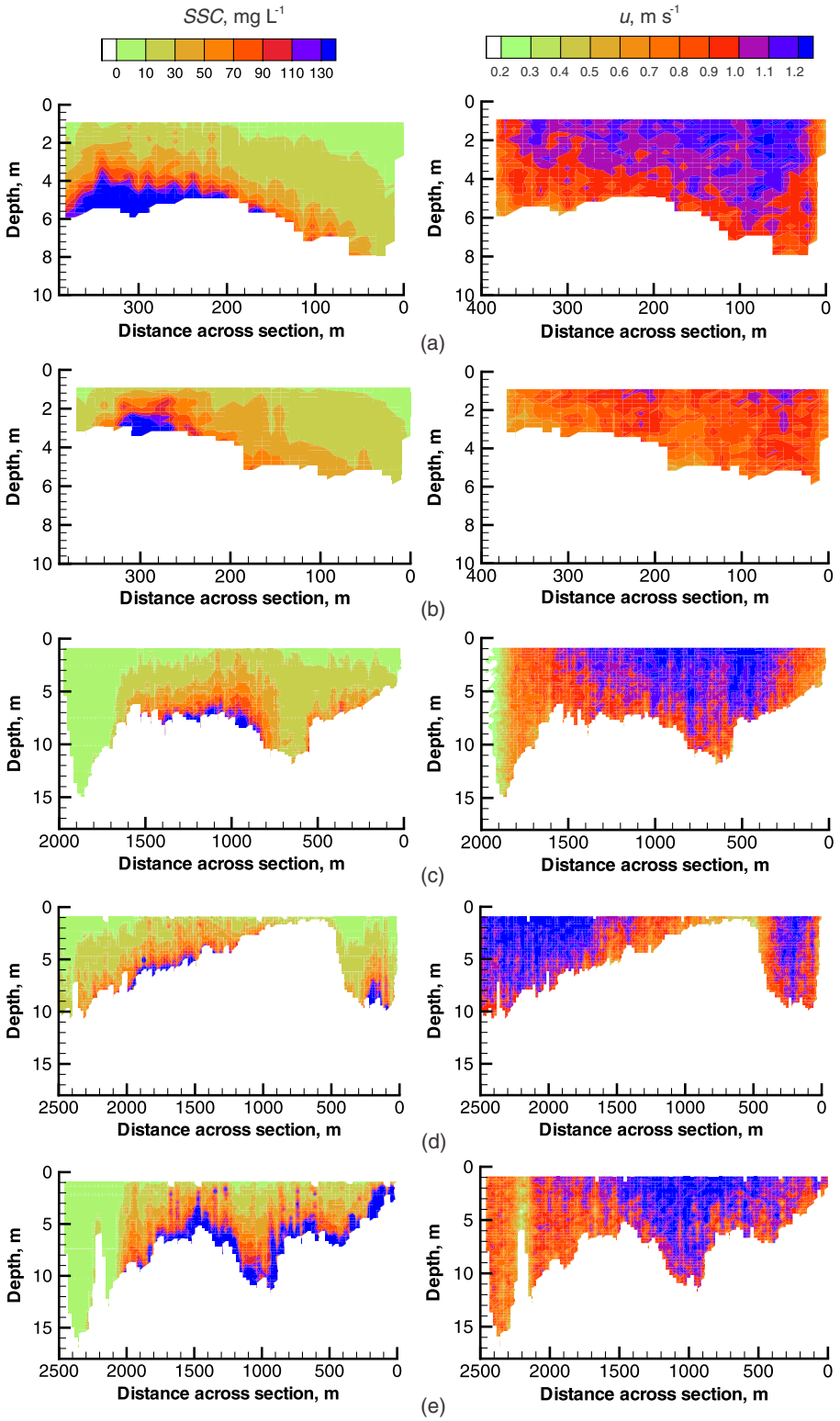

Fig. 10. Fields of flow velocity and suspended sand concentrations at different cross sections of (a and b) Zone C; (c–e) Zone A (distance across section: from left to right bank)

thus showing the small effects of bias errors on the calibration procedure. Moreover, the reasonable differences between sampled and computed values of total suspended bed-sediment transport (see next section) also support good estimation of suspended bed-sediment concentration across the different vertical locations.

Comparison of Suspended Load Estimations with Sampling and ADCP Profiling Methods

The calibration curve [Eq. (14)] was applied to estimate the suspended bed-sediment concentration (SSC) from the acoustic raw signal at each study section (and at each cell measured by the ADCP). Fluid absorption, beam spreading, and sediment attenuation were considered within each ADCP-measured cell at each cross section. The correction of fine sediment attenuation was applied considering a homogenous distribution of washload in the water column and across each section (using a mean value of $\overline{Cw}$ sampled at each field campaign). The coarse (sand) attenuation coefficient was computed at each cell, from the surface to the bottom, with Eq. (8) through a simple iterative solution. The concentration above each cell on the water column was computed through an integration of the above computed concentration cells and, therefore, considering a distribution of the bed-sediment concentrations along the water column. Table 5 summarizes the mean load estimations of suspended sand $\overline{\text{Gss}}_m$ applying the sampling and the proposed ADCP profiling method at two zones: Zone C (Colastine River) for two flow conditions and Zone A (Parana main channel) for three flow conditions (see Fig. 1 and Table 5). Note that $\overline{\text{Gss}}_m$ from the ADCP profiling method corresponds to an average of the four transects made at each cross section (only two at section A3). In addition to the sources of errors described above, the different spatial resolution from ADCP and classical approach to compute $\overline{\text{Gss}}_m$ could affect and increase the observed deviations in the load estimates detailed in Table 5. Note that the same amounts of depth-integrated samples (eight per cross section) were taken at the Colastine River (mean width of 360 m) and the Parana main channel (mean width of 2,000 m). More data and analyses should be considered in future studies to evaluate this effect. The underestimation in the Colastine River (C1 and C2) and the overestimation in the Parana (A1, A2, and A3) could be produced by this factor.

In addition to the above results regarding suspended bed-sediment transport across a section, Fig. 10 shows the suspended sand concentration field and the flow velocity field across the five studied cross sections. The high spatial resolution implies a significant advance in the knowledge of morphodynamic phenomena in large rivers (Szupiany et al. 2009, 2012).

Exposure Time versus Sediment Transport Difference

The exposure time criterion applied by Oberg and Mueller (2007) and Czuba and Oberg (2008) to identify the time needed to obtain accurate values of flow discharge was used to test the number of transects necessary to obtain reliable values of the suspended bed-sediment load at the five cross sections of Fig. 10. Results are shown in Fig. 11. The differences of the suspended load computed from an individual transect and the averages of two and three transects, with respect to the mean value obtained with four transects, are presented on the y-axis. Note that at section A3 only two transects were done; thus, one exposure time was plotted. The x-axis is the exposure time defined as the total amount of time spent sampling (or measuring) the flow discharge during a discharge measurement and includes neither time between transects nor time spent during moving bed tests or other tasks [Office of Surface Water (OSW) 2011]. It is seen that two transects would be enough in order to

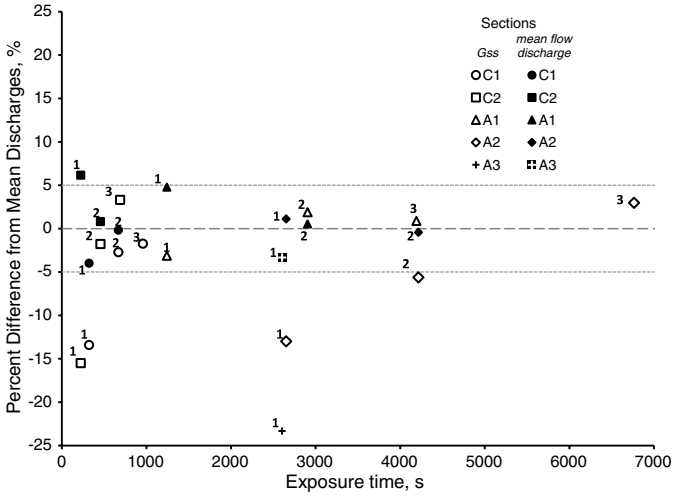

Fig. 11. Differences in the suspended load computed with one, two, and three transects respecting the average of four transects versus exposure time

have differences of ±6% with the mean suspended load obtained from the average of four transects. For individual transects, the differences are 13% (section C1), 16% (C2), 4% (A1), 13% (A2), and 23% (A3). These values could be affected by a bias error in flow discharge measurement. In order to separate the uncertainty in the velocity measurements and the concentration measurements, respectively, the exposure time criterion, considering only an even number of transects, was also applied to flow discharge and added in Fig. 11. When an even number of transects are considered, all values of $\overline{\text{Gss}}_m$ and Q are between ±6% suggesting that the same criterion could be applied for both variables.

Sensitivity Analysis of the Suspended Load Estimations to Variations of Calibration Parameters

The calibration of the backscatter signal and the subsequent suspended load estimations required many input parameters that had to be defined in advance [see Eqs. (3)–(8)]. The accurate definitions of instrument parameters (e.g., acoustic frequency, bin size, transducer radius and depth) and of those related to the suspended sediment (e.g., mean concentrations and grain size) affect the final results. In particular, mean concentration and grain size are often poorly known in natural rivers. To see how the uncertainties in the selection of some of these parameters affect the estimations of suspended loads ($\overline{\text{Gss}}_m$), a sensitivity analysis was performed on changes in (1) the fine and coarse sediment grain sizes (D_f and D_g, respectively); (2) the concentrations of fine material; and (3) the transducer depth (r_t). They were varied up to ±100% with respect to the values used to estimate $\overline{Gss}_m$ at cross sections A1 and C1 [Figs. 12(a and b)]. The dashed box in Fig. 12 shows the effects on $\overline{\text{Gss}}_m$ due to deviations of ±50% in the selected values of the parameters. The sensitivity analysis shows that (1) underestimations of fine material grain size were associated with maximum errors of $\overline{\text{Gss}}_m$ (19 and 33% for the Colastine and Parana Rivers, respectively) which is reflected by increasing values of the α_{sf} coefficient [Eq. (8) and Fig. 2] and, therefore, higher values of CSCM [Eq. (12)] and of SSC [Eq. (14)]; (2) variations of the fine sediment concentrations affected the estimations of suspended loads up to 15% [Fig. 12(b)]; (3) errors in the measurement of the transducer depth yielded deviations up to 15% in the suspended loads [Fig. 12(a)] because the acoustic path range varies and it hinders the assessment of transmission losses [Eq. (3)]; and (4) the diameter

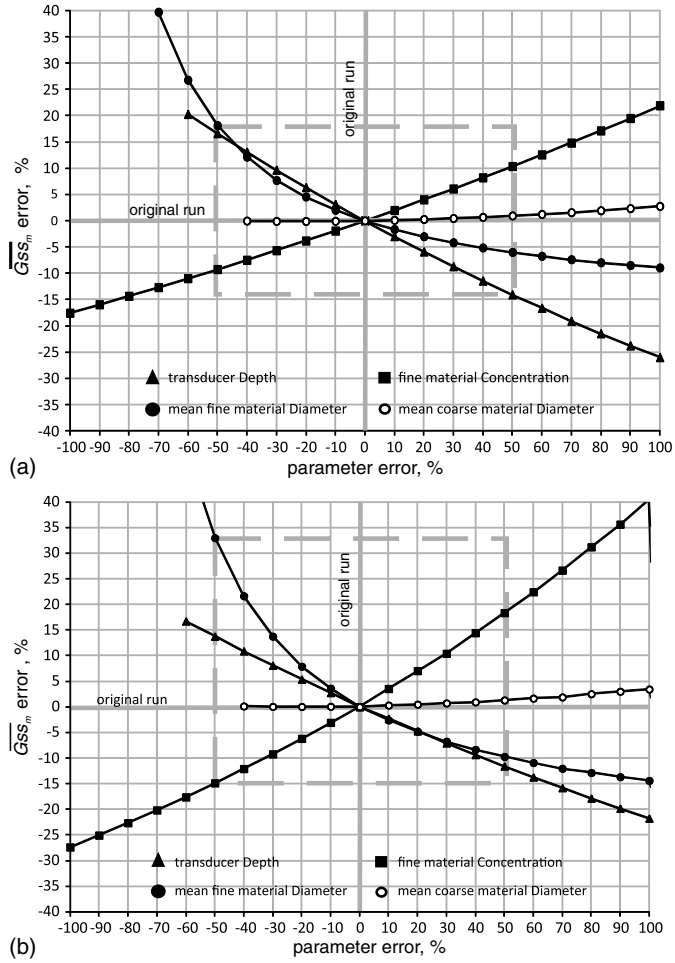

Fig. 12. Sensitivity of $\overline{\mathrm{Gss}}_m$ to variations of several input parameters at the cross sections of the (a) Colastine River; and (b) Parana River (dashed box corresponds to ±50% variation)

of coarse sediment slightly affected the final load of suspended sediment because the corresponding attenuation coefficient [Eq. (8)] is very small (Table 3).

This sensitivity analysis highlights the importance of properly knowing the required parameters before applying any ADCP-sediment calibration, especially the suspended sediment characteristics because they produce changes in the attenuation behaviors. Although estimated $\overline{\mathrm{SSC}}$ values are less affected by attenuation effects, as demonstrated in the previous section, the value of $\overline{\mathrm{Gss}}_m$ involves the sum of all errors in the estimated SSC value at each cell, and thus this error becomes more important in large rivers.

Conclusions

The ADCP is a valuable tool for monitoring the suspended sediment load in large rivers where standard sampling methods used to determine the field of suspended transport across an entire cross section are labor intensive, unsafe, costly, and time consuming. The suspended bed-sediment transport values estimated applying the ADCP profiling and water column sampling methods differ less than 46% in the investigated cross sections. These deviations appear low if compared with current variations in results of sediment transport studies (around 100%). Additional important advantages of the ADCP profiling method are shorter measurement processing time, lower operating costs, and high spatial and temporal resolution of measurements that enable the investigation of hydro-sedimentological processes in large natural channels, which nowadays are hard to undertake.

Despite all the assumptions involving the use of depth-integrated sediment samplers, it has been shown that it is a valuable and useful sampler for this type of acoustic calibration in large rivers. This has a great impact on the research and engineering community working in large rivers, because depth-integrated sediment samplers present some important operational advantages in comparison with point samplers (i.e., shorter measuring time, lower amount of sediment samples and processing time in laboratory, and therefore, lower field and laboratory costs).

A successful calibration was achieved between the concentrations of suspended sand and the backscattered signal of the ADCP. The value of the regression slope was in the order of the theoretical value [0.1 in Eq. (2)] with $R^2 = 0.91$ [Fig. 7, Eq. (13)]. The scatter of the point data was less than ±20%. The dispersion sources do not produce strong scatter or bias error on the results, with acceptable uncertainty of suspended bed-sediment concentration for this poorly known variable in large streams. Though the concentration of washload (silt and clay) is two to ten times higher than the sand concentration at the cross sections studied herein, the fine material does not correlate with the backscatter signal (Fig. 8).

As long as the concentration and the fraction of suspended material remain in the range of the observed values ($\overline{Cw} < 200\ \mathrm{mg\,L^{-1}}$ and $\overline{\mathrm{SSC}} < 100\ \mathrm{mg\,L^{-1}}$), the sound absorption due to water viscosity is larger than that due to sediment attenuation, and among different grain sizes, fine sediment gives rise to larger attenuation. It has been shown that signal backscatter is governed by the coarse particles with no significant influence of the fine material, as reported by different authors (e.g., Topping et al. 2007; Wright et al. 2010). The mentioned findings support the small influence of the proposed assumption (and used sampler) (i.e., monosized suspended bed sediment and homogeneous distribution of suspended bed sediment). Further analyses are needed for different conditions such as grain size, highest fine and coarse material concentrations, and concentration ratios between fine and coarse material using instruments with different acoustic frequency. These factors could affect/modify the roles of backscatter and absorption presented in this paper.

The analysis presented in Fig. 11 suggests that the same exposure time criterion adopted by the USGS (Oberg and Mueller 2007; Czuba and Oberg 2008; OSW 2011) to obtain accurate discharge values is valid for suspended load computed from the methodology proposed in this paper. Note that if we consider values of exposure time higher than 720 s (OSW 2011) and, at least, the average value of two transects, the differences are below 6% for the studied sections. An even number of transects with reciprocal courses is required to minimize directional bias in measured discharge (OSW 2011).

A sensitivity analysis on the selected values of sediment grain sizes and concentrations for the preliminary assessment of sound absorptions showed that 50% variations correspond to 30% deviation in the resulting sediment transport. The sensitivity analysis showed that it is necessary to have accurate knowledge of the values of the variables required for the calibration and use of the proposed experimental method to estimate sediment transport using ADCP. These required variables include a representative size of fine and coarse suspended materials and fine sediment concentrations, variables that are generally poorly recorded in natural streams. It is also recommended to perform the fine sediment sampling in order to be applied to the calibration of ADCP recording.

Finally, it is noteworthy that all large rivers in the world present similar mean slope energy and mean bed-sediment size values

(see Table 2 from Latrubesse 2008), suggesting that a direct extrapolation of the presented methodology could be applied to other large rivers, with a great impact on the research and engineering community working at such large scales.

Acknowledgments

The authors thank Roberto Mir and Santiago Cañete for their assistance during the field work. This study is part of project PICT 2006-00758, "Measurement and calculation of river sediment transport" funded by the Agencia Nacional de Promoción Científica y Tecnológica of Argentina and project CAID 2009 "Analysis of morphodynamics processes in a floodplain of a large lowland river: The Parana river in its middle reach" funded by the Universidad Nacional del Litoral of Argentina.

Notation

The following symbols are used in this paper:

a = reference level in Rouse equation;
a_s = particle radius;
a_t = transducer radius;
CSB = corrected signal for the effect of beam spreading;
CSCM = corrected signal for attenuation of coarse material;
$\overline{\text{CSCM}}$ = depth-average corrected signal for attenuation of coarse material;
CSF = corrected signal for the effect of fluid absorption;
CSFM = corrected signal for attenuation of fine material;
Cw = washload;
$\overline{\text{Cw}}$ = depth-integrated washload;
c = speed of sound in water;
D = particle diameter;
D_f = mean fine material diameter;
D_g = mean coarse material diameter;
f = acoustic frequency;
f_s = form function that describes the scattering properties of the particles;
f_T = temperature-dependent relaxation frequency;
Gss = suspended bed-sediment transport;
$\overline{\text{Gss}}_m$ = mean suspended bed-sediment transport at cross section;
H_B = bin size;
h = mean flow depth;
K_T = global constant;
K_t = instrument-specific system constant;
k = wave number;
M = mass concentration;
Q = water discharge;
RL = raw signal strength (reverberation level);
r = slant distance from transducer to center of bin;
r_t = transducer depth;
r_0 = range;
S = sediment relative density;
SL = source level;
SSC = suspended sand concentration;
$\overline{\text{SSC}}$ = depth-integrated suspended sand concentration;
$\overline{\text{SSC}}_i$ = mean suspended sand concentration within a subsection;
T = temperature;
$2TL$ = correction of transmission losses;
$\bar{U}$ = mean flow velocity within a subsection;
u = mean flow velocity;
u_* = shear velocity;
z = Rouse equation parameter;
α = attenuation and absorption coefficient;
α_f = absorption coefficient;
α_s = attenuation coefficient;
α_{sf} = attenuation coefficient due to fine material;
α_{sg} = attenuation coefficient due to coarse material;
λ = acoustic wavelength;
ρ = water density;
ρ_s = particle density;
σ_g = geometric deviation;
τc = pulse length;
ν = kinematic viscosity;
ψ = coefficient of transducer near-field correction; and
Ω_i = subarea into a cross section.

References

Alarcon, J., Szupiany, R., Montagnini, M., Gaudin, H., Prendes, H., and Amsler, M. (2003). "Evaluación del transporte de sedimentos en el tramo medio del río Paraná." *Proc., Primer Simposio Regional sobre Hidráulica de Ríos*, Instituto Nacional del Agua, Buenos Aires, Argentina, 1–2.

Czuba, J. A., and Oberg, K. A. (2008). "Validation of exposure time for discharge measurements made with two bottom-tracking acoustic Doppler current profilers." *Proc., IEEE/OES/CMTC 9th Working Conf. on Current Measurement Technology*, Current Measurement Technology Committee of the Oceanic Engineering Society Institute of Electrical and Electronics Engineers, Piscataway, NJ, 250–257.

Deines, K. L. (1999). "Backscatter estimation using broadband acoustic Doppler current profilers." *Proc., IEEE/OES/CMTC 6th Working Conf. on Current Measurement Technology*, Current Measurement Technology Committee of the Oceanic Engineering Society Institute of Electrical and Electronics Engineers, Piscataway, NJ, 249–253.

Dinehart, R. L., and Burau, J. R. (2005). "Averaged indicators of secondary flow in repeated acoustic Doppler current profiler crossing of bends." *Water Resour. Res.*, 41(9), 1–18.

Downing, A., Thorne, P. D., and Vincent, C. E. (1995). "Backscattering from a suspension in the near-field of a piston transducer." *J. Acoust. Soc. Am.*, 97(3), 1614–1620.

Drago, E., and Amsler, M. L. (1988b). "Suspended sediment at a cross section of the Middle Parana River: Concentration, granulometry and influence of main tributaries." *Proc., Symp. on Sediment Budgets*, Vol. 174, International Association of Hydrological Sciences, Wallingford, Oxfordshire, 381–396.

Drago, E., and Amsler, M. L. (1998). "Bed sediment characteristics in the Parana and Paraguay rivers." *Water Int.*, 23(3), 174–183.

Fulford, J. M., and Sauer, V. B. (1986). "Comparison of velocity interpolation methods for computing open-channel discharge." *Hydrologic Sciences*, S.Y. Subitsky, ed., U.S. Geological Survey Water-Supply, Washington, 154.

García, M. H. (2008). "Sediment transport and morphodynamics." Chapter 2, *Sedimentation engineering: Processes, measurements, modelling and practice*, M. H. García, ed., ASCE, Reston, VA, 111–114.

Gartner, J. W. (2004). "Estimating suspended solids concentrations from backscatter intensity measured by acoustic Doppler current profiler in San Francisco Bay, California." *Mar. Geol.*, 211(3–4), 169–187.

Giacosa, R., Paoli, C., and Cacik, P. (2000). "El Río Paraná en su Tramo Medio." Chapter 2, *Conocimiento del Régimen Hidrológico*, C. Paoli and M. Schreider, eds., Centro de Publicaciones, Universidad Nacional del Litoral, Santa Fe, Argentina, 71–103.

Gray, J. R., and Gartner, J. W. (2009). "Technological advances in suspended-sediment surrogate monitoring." *Water Resour. Res.*, 45(4), W00D29.

Gray, J. R., Glysson, D., and Edwards, T. (2008). "Suspended-sediment samplers and sampling methods." Chapter 5, *Sedimentation engineering—Processes, measurements, modeling, and practice*, M. García, ed., ASCE, Reston, VA, 320–353.

Gray, J. R., and Simões, F. J. M. (2008). "Estimating sediment discharge." *Sedimentation engineering—Processes, measurements, modeling, and practice*, M. García, ed., ASCE, 1067–1088.
Guerrero, M., Rüther, N., and Szupiany, R. N. (2012). "Laboratory validation of ADCP techniques for suspended sediments investigation." *Flow Meas. Instrum.*, 23(1), 40–48.
Guerrero, M., Szupiany, R. N., and Amsler, M. (2011). "Comparison of acoustic backscattering techniques for suspended sediments investigation." *Flow Meas. Instrum.*, 22(5), 392–401.
Guerrero, M., Szupiany, R. N., and Latosinski, F. (2013). "Multi-frequency acoustics for suspended sediment investigation: Validation in the Parana River." *J. Hydraul. Res.*, 51(6), 696–707.
Guy, H. P., and Norman, V. W. (1970). "Fluvial sediment concepts." Chapter C1, *Techniques for water resources investigations of the U.S. Geological Survey*, USGS, Arlington, VA.
Hanes, D. M. (2012). "On the possibility of single-frequency acoustic measurement of sand and clay concentrations in uniform suspensions." *Cont. Shelf Res.*, 46, 64–66.
Hoitink, A., and Hoekstra, P. (2005). "Observations of suspended sediment from ADCP and OBS measurements in a mud-dominated environment." *Coastal Eng.*, 52(2), 103–118.
Holdaway, G. P., Thorne, P. D., Flatt, D., Jones, S. E., and Prandle, D. (1999). "Comparison between ADCP and transmissometer measurement of suspended sediment concentration." *Cont. Shelf Res.*, 19(3), 421–441.
Latrubesse, E. (2008). "Patterns of anabranching channels: The ultimate end-member adjustments of mega-rivers." *Geomorphology*, 101(1–2), 130–145.
Mangini, S. P., Prendes, H. H., Amsler, M. L., and Huespe, J. (2003). "Importancia de la floculación en la sedimentación de la carga de lavado en ambientes del Río Paraná." *Revista Ingeniería Hidráulica En México*, XVIII(3), 55–69.
Moate, B. D., and Thorne, P. D. (2012). "Interpreting acoustic backscatter from suspended sediments of different and mixed mineralogical composition." *Cont. Shelf Res.*, 46, 67–82.
Montagnini, M. D., Prendes, H. H., Schreider, M. I., Amsler, M. L., and Martinez, H. L. (1998). "Desarrollo de un muestreador de sedimentos en suspensión integrador en profundidad." *Proc., XVII Congreso Nacional del Agua*, Santa Fe, Argentina, III, 535–537.
Moore, S. A., Le Coz, J., Hurther, D., and Paquier, A. (2012). "On the application of horizontal ADCPs to suspended sediment transport surveys in rivers." *Cont. Shelf Res.*, 46, 50–63.
Oberg, K. A., and Mueller, D. S. (2007). "Analysis of exposure time on streamflow measurements made with acoustic Doppler current profilers." *Proc., Hydraulic Measurements and Experimental Methods Conf.*, ASCE, Reston, VA, 6.
Office of Surface Water (OSW). (2011). "Exposure time for ADCP moving-boat discharge measurements made during steady flow conditions." *Technical Memorandum 2011.08*, U.S. Geological Survey, Reston, VA.
Parsons, D. R., et al. (2013). "Velocity mapping toolbox (VMT): A new post-processing suite for acoustic Doppler current profiler data." *Earth Surf. Processes Landforms*, 38(11), 1244–1260.
Prendes, H. H., Mangini, S. P., and Huespe, J. (2009). "Deposition of fine sediments in ports and navigation channels in Paraná River." *Proc., 10th Int. Conf. on Cohesive Sediment Transport Processes*, Laboratory of Cohesive Sediment Dynamics-Universidad Federal de Río de Janeiro, Rio de Janeiro, Brazil.
RD Instruments. (1999). "Using the 305A4205 hydrophone to identify the RSSI scale factors for calibrating the echo strength output of an ADCP." *Technical note, FST-004*, RD Instrument, San Diego, CA.
Reichel, G., and Nachtnebel, H. P. (1994). "Suspended sediment monitoring in a fluvial environment—Advantages and limitations applying an acoustic-Doppler-current-profiler." *Water Res.* 28(4), 751–761.
Sassi, M. G., Hoitink, A. J. F., and Vermeulen, B. (2012). "Impact of sound attenuation by suspended sediment on ADCP backscatter calibrations." *Water Resour. Res.*, 48(9), W09520.
Schulkin, M., and Marsh, H. W. (1962). "Sound absorption in sea water." *J. Acoust. Soc. Am.*, 34(6), 864–865.
Simpson, M. R. (2001). "Discharge measurements using a broad-band acoustic Doppler current profiler." *Open File Report 01-1*, USGS, Sacramento, CA.
Szupiany, R. N., et al. (2012). "Flow fields, bed shear stresses, and suspended bed sediment dynamics in bifurcations of a large river." *Water Resour. Res.*, 48(11), W11515.
Szupiany, R. N., Amsler, M. L., Best, J. L., and Parsons, D. R. (2007). "Comparison of fixed- and moving vessel measurements with an ADP in a large river." *J. Hydraul. Eng.*, 10.1061/(ASCE)0733-9429(2007)133:12(1299), 1299–1309.
Szupiany, R. N., Amsler, M. L., Parsons, D. R., and Best, J. L. (2009). "Morphology, flow structure and suspended bed sediment transport at two large braid-bar confluences." *Water Resour. Res.*, 45(5), W05415.
Teledyne RD Instruments. (2007). "Work Horse Rio Grande ADCP User's Guide." *Publication Number 957-6167-00*, Teledyne RDI Instruments, Poway, CA, 28.
Thevenot, M. M., Prickett, T. L., and Kraus, N. C. (1992). "Tylers Beach, Virginia, dredged material plume monitoring project 27 September to 4 October 1991." Dredging research program, *Technical Rep. DRP-92-7*, U.S. Army Corps of Engineers, Washington, DC, 204.
Thorne, P. D., and Hanes, D. M. (2002). "A review of acoustic measurements of small-scale sediment processes." *Cont. Shelf Res.*, 22(4), 603–632.
Thorne, P. D., and Meral, R. (2008). "Formulations for the scattering properties of suspended sandy sediments for use in the application of acoustics to sediment transport processes." *Cont. Shelf Res.*, 28(2), 309–317.
Topping, D. J., Rubin, D. M., Wright, S. A., and Melis, T. S. (2011). "Field evaluation of the error arising from inadequate time averaging in the standard use of depth-integrating suspended-sediment samplers." *Professional Paper 1774*, USGS, Reston, VA, 95.
Topping, D. J., Wright, S. A., Melis, T. S., and Rubin, D. M. (2007). "High-resolution measurements of suspended-sediment concentration and grain size in the Colorado River in Grand Canyon using a multi-frequency acoustic system." *Proc., 10th Int. Symp. on River Sedimentation*, M. V. Lomonosov, Moscow State Univ., Moscow, Russia.
Trento, A. E., Amsler, M. L., and Pujol, A. (1990). "Perfiler observados de velocidad en un tramo del río Paraná—Analisis Teorico." *Proc., XIV Congreso Latinoamericano de Hidráulica*, Montevideo, Uruguay.
Urick, R. J. (1948). "The absorption of sound in suspensions of irregular particles." *J. Acoust. Soc. Am.*, 20(3), 283–289.
Vanoni, V. A. (1975). "Sediment measurement techniques. Fluvial Sediment." Chapter III-A, *Sedimentation engineering, ASCE-manuals and reports on engineering practise-N°54*, V. A. Vanoni, ed., ASCE, Reston, VA, 317–321.
Wall, G. R., Nystrom, E. A., and Litten, S. (2006). "Use of an ADCP to compute suspended sediment discharge in the Tidal Hudson River, New York." *Scientific Investigations Report 2006–5055*, USGS, Reston, VA.
World Meteorological Organization (WMO). (1994). "Guide to hydrological practices." *Data acquisition and processing, analysis, forecasting and other applications*, 5th Ed., Geneva, 176–178.
Wright, S. A., Topping, D. J., and Williams, C. A. (2010). "Discriminating silt-and-clay from suspended-sand in rivers using side-looking acoustic profilers." *Proc., 2nd Joint Federal Interagency Conf.*, Advisory Committee on Water Information, Reston, VA.